

PLANT SCIENCE

Root branching toward water involves posttranslational modification of transcription factor ARF7

Beatriz Orosa-Puente^{1*†}, Nicola Leftley^{2†}, Daniel von Wangenheim^{2†}, Jason Banda², Anjil K. Srivastava¹, Kristine Hill^{2†}, Jekaterina Truskina^{2,3}, Rahul Bhosale², Emily Morris², Moumita Srivastava¹, Britta Kümpers², Tatsuaki Goh^{2,4§}, Hidehiro Fukaki⁴, Joop E. M. Vermeer^{5,6}, Teva Vernoux³, José R. Dinneny⁷, Andrew P. French^{2,8}, Anthony Bishopp², Ari Sadanandom^{1¶}, Malcolm J. Bennett^{2¶}

Plants adapt to heterogeneous soil conditions by altering their root architecture. For example, roots branch when in contact with water by using the hydropatterning response. We report that hydropatterning is dependent on auxin response factor ARF7. This transcription factor induces asymmetric expression of its target gene *LBD16* in lateral root founder cells. This differential expression pattern is regulated by posttranslational modification of ARF7 with the small ubiquitin-like modifier (SUMO) protein. SUMOylation negatively regulates ARF7 DNA binding activity. ARF7 SUMOylation is required to recruit the Aux/IAA (indole-3-acetic acid) repressor protein IAA3. Blocking ARF7 SUMOylation disrupts IAA3 recruitment and hydropatterning. We conclude that SUMO-dependent regulation of auxin response controls root branching pattern in response to water availability.

The soil resources plants require, such as water, are often distributed heterogeneously (1). To aid foraging, root development is responsive to the spatial availability of soil signals (2, 3). Microcomputed tomography imaging revealed that soil-water contact affects root architecture, causing lateral roots (LRs) to form when roots are in direct contact with moisture (4, 5). This adaptive branching response is termed hydropatterning (4, 5). In this current study, we report the molecular mechanism controlling hydropatterning, revealing that core components of the auxin response machinery are targets for posttranslational regulation.

The hydropatterning response can be mimicked in vitro by growing seedling roots vertically on the surface of agar plates (4). Opposite sides of

a root are either in contact with moisture (directly with the plate or via the meniscus) or exposed to air (fig. S1). To visualize whether primordia preferentially form on the side in contact with moisture, we transferred a root, including the gel it was growing on, into a light sheet fluorescence microscope to image young primordia and measure their angle of outgrowth with respect to the agar surface (fig. S1). This revealed that LRs preferentially emerge from the side of the root in contact with moisture (Fig. 1A).

What causes new primordia to form on the water-contact side of a root? Seedlings exposed to a hydropatterning stimulus exhibit an auxin response gradient across the root radius (4). Auxin regulates LR development (6). Auxin-responsive gene expression is regulated by a family of transcription factors termed auxin response factors (ARFs) (7). The model plant *Arabidopsis thaliana* contains five *ARF* transcriptional activating genes termed *ARF5*, -6, -7, -8, and -19 (8). To determine which *ARF* gene(s) controls hydropatterning, we phenotyped loss-of-function alleles. *ARF7* mutants (8, 9) were all impaired (Fig. 1, A to C, and fig. S2), whereas hydropatterning was normal in mutants of other *ARF* family members tested (fig. S3). Hence, hydropatterning appears *ARF7* dependent.

ARF7 regulates LR initiation (6, 8, 10, 11). Network inference, chromatin immunoprecipitation-polymerase chain reaction (ChIP-PCR) validation, and transcriptomic studies have revealed that *ARF7* controls the auxin-dependent expression of LR regulatory genes such as *LBD16* (fig. S4) (12). Like *ARF7*, *LBD16* loss-of-function alleles *lbd16-1* and *lbd16-2* exhibit a hydropatterning defect (fig. S5). *ARF7* may therefore

control hydropatterning in an *LBD16*-dependent manner. *LBD*-like genes are differentially expressed in maize during hydropatterning (5). To determine whether *LBD16* is differentially expressed in response to a hydropatterning stimulus by *ARF7*, we monitored spatial expression of a *gLBD16-green fluorescent protein (GFP)* reporter (13). *LBD16-GFP* was first detected in the elongation zone (Fig. 1D and movie S1) in a subset of cells [termed xylem pole pericycle (XPP) founder cells, from which primordia originate], consistent with this reporter being an early marker for LR development (13). In *Arabidopsis*, LRs originate from pericycle cells positioned above either xylem pole (6). We tested whether *gLBD16-GFP* was differentially expressed in XPP cell files closest to the agar. To mark which side of a root was exposed to air, we overlaid samples with agar with a low melting point and containing fluorescent beads and then imaged from multiple angles using light sheet microscopy (figs. S6 to S8). Reconstructed root images revealed preferential *gLBD16-GFP* expression in XPP cell nuclei earlier on one side of wild-type (WT) roots (Fig. 1E). Asymmetric *gLBD16-GFP* expression was disrupted in *arf7-1* (Fig. 1F), consistent with the mutant's hydropatterning defect (Fig. 1C). Quantification of *LBD16-GFP* distribution in WT and *arf7-1* revealed this reporter was differentially expressed in an *ARF7*-dependent manner (fig. S8, A to D and F). To test whether asymmetric *LBD16* expression is essential for hydropatterning, the constitutive 35S promoter was used to drive *LBD16* expression in *lbd16* (fig. S9). Expression of 35S:*LBD16* failed to rescue the *lbd16* hydropatterning defect (in contrast to *LBD16:LBD16-GFP*). Hence, asymmetric *LBD16* expression is essential for hydropatterning.

We next tested whether *LBD16*-dependent hydropatterning was controlled by means of differential *ARF7* expression by using transcriptional and translational *ARF7pro::ARF7-VENUS* reporters (figs. S10 and S11). In contrast to *gLBD16-GFP* (Fig. 1, E and F), *ARF7* reporters did not exhibit differential expression in LR stem cells (Fig. 1G). To test whether *ARF7* was a target of posttranslational regulation, *ARF7* was constitutively expressed (using the 35S promoter) in *arf7-1*. This revealed 35S:*ARF7* could rescue *arf7-1* hydropatterning (Fig. 1C and fig. S12). Hence, *ARF7* appears to control hydropatterning by means of a posttranslational (rather than transcriptional) mechanism.

ARF7 contains posttranslational regulatory motifs including four putative sites for addition of small ubiquitin-like modifier (SUMO) proteins at lysine residues (K104, K151, K282, and K889) (Fig. 2A). SUMO, unlike ubiquitin, can modify the function (rather than abundance) of target proteins (14). We confirmed *ARF7* is a target for SUMOylation by coexpressing GFP- and hemagglutinin (HA) epitope-tagged *ARF7* and SUMO sequences (Fig. 2B). Addition of SUMO to *ARF7* is abolished after replacing lysine with arginine in all four *ARF7* SUMOylation motifs (in *gARF7^{4K/R}*; Fig. 2B).

¹Department of Biosciences, University of Durham, Durham DH1 3LE, UK. ²Plant and Crop Sciences, School of Biosciences, University of Nottingham, Sutton Bonington LE12 5RD, UK. ³Laboratoire Reproduction et Développement des Plantes, Univ Lyon, ENS de Lyon, F-69342, Lyon, France.

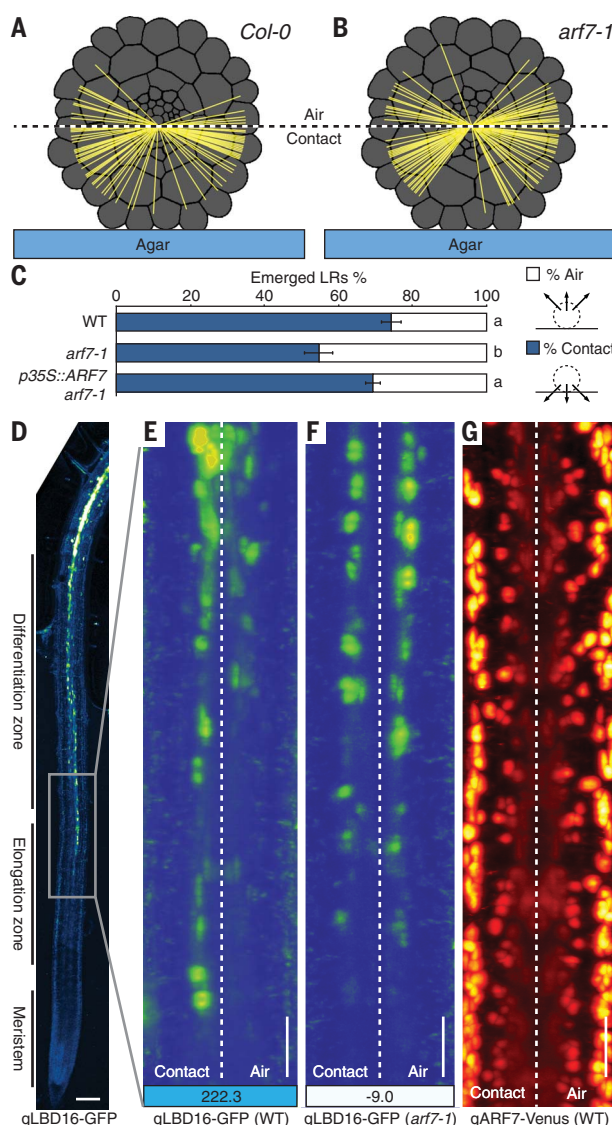
⁴Department of Biology, Graduate School of Science, Kobe University, Kobe 657-8501, Japan. ⁵Department of Plant and Microbial Biology, University of Zurich, CH-8008 Zurich, Switzerland. ⁶Developmental Biology, Wageningen University and Research, Wageningen, Netherlands. ⁷Department of Biology, Stanford University, Stanford, CA 94305, USA.

⁸School of Computer Science, Jubilee Campus, University of Nottingham, Nottingham NG8 1BB, UK.

*Present address: School of Biological Sciences, University of Edinburgh, Edinburgh EH9 3FF, UK. †These authors contributed equally to this work. ‡Present address: Center for Plant Molecular Biology – ZMBP, University of Tübingen, D - 72076 Tübingen, Germany. §Present address: Graduate School of Science and Technology, Nara Institute of Science and Technology, 8916-5 Takayama, Ikoma 630-0192, Japan. ¶Corresponding author. Email: ari.sadanandom@durham.ac.uk (A.S.); malcolm.bennett@nottingham.ac.uk (M.J.B.)

Fig. 1. *Arabidopsis* root branching toward water is ARF7 dependent.

(A and B) Cross-section schematic of a root growing on agar. The LR primordia outgrowth angle (yellow lines) in respect to the agar surface is quantified from 3D light sheet microscopy images of WT (A) and *arf7-1* (B) plants. (C) Hydropatterning bioassay of WT, *arf7*, and *arf7* overexpressing ARF7 (p35S::ARF7). Data shown are mean values \pm SE. Statistical differences were analyzed on the percent of emerged LRs emerging toward either contact or air using an analysis of variance, Tukey's HSD test ($P < 0.05$); statistically similar groups are indicated using the same letter. (D) Confocal image of *Arabidopsis* root tip expressing *gLBD16-GFP*. Gray boxed area highlights onset of *LBD16-GFP* expression in the elongation zone. (E to G) Maximum intensity projections of radial reslices obtained from light sheet fluorescent microscopy-multiview imaging show the gene expression pattern of *LBD16-GFP* in WT (E), *arf7* (F), and *ARF7::ARF7-Venus* (G) on the contact versus air sides. The numbers at the bottom of (E) and (F) display the index of asymmetry. Positive values correspond to an earlier expression beginning on the contact side; negative values show asymmetry toward the air side. Details are explained in figs. S1 and S6 to S8. Scale bars, 50 μ m.



To test the importance of ARF7 SUMOylation for LR development and hydropatterning, we expressed SUMOylatable *gARF7* and non-SUMOylatable *gARF7^{4K/R}* transgenes in *arf7-1*. Bioassays revealed *arf7* hydropatterning could be rescued by WT *gARF7* (Fig. 2, C and D, and fig. S13) but not by *gARF7^{4K/R}* (Fig. 2, E and F, and fig. S14). Nevertheless, *gARF7^{4K/R}* (like *gARF7*) remained capable of restoring *arf7* LR density to a WT level (Fig. 2F). Hence, ARF7^{4K/R} remained functional but unable to regulate hydropatterning. Quantification of *LBD16-GFP* distribution in *gARF7* versus *gARF7^{4K/R} arf7-1* revealed that this reporter was differentially expressed only in the presence of SUMOylatable ARF7 (fig. S8, A to C and E and G). We conclude ARF7 SUMOylation is required for hydropatterning.

How does SUMOylation modify ARF7 activity? ARF7 is rapidly SUMOylated after auxin treatment (Fig. 2G). One ARF7 SUMOylation

site (K151) is located within the DNA binding domain (Fig. 2A) (15). SUMOylation may attenuate auxin-induced ARF7 DNA binding activity. Time course ChIP-PCR analysis revealed ARF7 transiently interacts with the *LBD16* promoter after auxin treatment (fig. S15). Furthermore, ChIP-PCR assays performed on *LBD16* and *LBD29* target promoters detected higher DNA binding by ARF7^{4K/R}-GFP than WT ARF7-GFP (fig. S16). Hence, SUMOylation negatively regulates ARF7 DNA binding activity.

ARF7 transcriptional activity is negatively regulated by Aux/IAA (indole-3-acetic acid) repressor proteins (16). Aux/IAA proteins such as IAA3/SHY2 and IAA14/SLR control ARF7 activity during LR development (16, 17). Like *arf7-1*, *IAA3* loss-of-function allele *shy2-31* causes an LR hydropatterning defect (Fig. 3A and fig. S17). Thus, we tested whether interactions among ARF7, IAA3/SHY2, and IAA14/SLR were SUMO

dependent. Pull-down assays revealed that ARF7-GFP interacted with IAA3/SHY2 and IAA14/SLR proteins (fig. S18). In contrast, non-SUMOylatable ARF7^{4K/R} largely failed to pull down IAA3/SHY2. However, both forms of ARF7 interacted with IAA14/SLR (fig. S19). Hence, interaction between ARF7 and IAA3/SHY2 (but not IAA14/SLR) depends on the residues that regulate ARF7 SUMOylation.

Bioinformatic analysis revealed that *IAA3/SHY2* (but not *IAA14/SLR*) contained a SUMO interaction motif (SIM) (Fig. 3B). With its SIM domain mutated, interaction between IAA3 and WT ARF7 was abolished (Fig. 3C). Nevertheless, the IAA3 SIM mutant protein could interact with the TIR1 auxin receptor and TPL transcriptional repressor (figs. S19 and S20). Hence, mutating the SIM site differentially affects IAA3's ability to interact with SUMOylated ARF7 but not with other partners.

To assess the functional importance of the *IAA3* SIM sequence in planta, we engineered transgenic plants overexpressing *shy2-2* with or without SIM sequences. We examined the impact of the SIM sequence on the suppression of root branching characteristic of *shy2-2* mutant plants (18), a phenotype not dependent on hydropatterning. We drove overexpression of the *shy2-2* gene with the endodermis-specific CASP promoter. More root branching is evident in roots of plants expressing *pCASP:shy2-2* without the SIM sequence than in plants expressing *pCASP:shy2-2* with the SIM sequence (Fig. 3D). Thus, overexpression of *shy2-2* in endodermis can block ARF7-dependent LR development, but only if the SIM sequence is included.

SUMO modifiers are added and removed from target proteins by E3 ligases and SUMO proteases, respectively. In *Arabidopsis*, OTS1 and OTS2 proteases cleave off SUMO from nuclear localized proteins (19). Pull-down assays revealed ARF7 is a direct target for OTS1 (fig. S21). Our bioassays revealed that the *ots1 ots2* mutant exhibits a hydropatterning defect (fig. S22). Hence, hydropatterning appears dependent on OTS1 and OTS2 function. These SUMO proteases are labile when plants are exposed to abiotic stress, causing their SUMOylated target proteins to accumulate (19, 20). Indeed, transiently exposing *gARF7-GFP* seedlings to 20 minutes outside an agar plate resulted in a rapid increase in ARF7 SUMOylation (Fig. 2H). Hence, the absence (rather than the presence) of water stimulates this posttranslational response. Modeling suggests a substantial differential in water potential is generated across the air and contact axis of the root (5). We hypothesize that this triggers SUMOylated ARF7 on the air side of roots to recruit IAA3 and create a transcriptional repressor complex, thereby blocking auxin-responsive gene expression associated with LR initiation (Fig. 3E). Conversely, because IAA3 cannot be recruited by non-SUMOylated ARF7 in root cells on the contact side, this population of transcription factors can induce expression of genes like *LBD16* to trigger organ initiation (Fig. 3E).

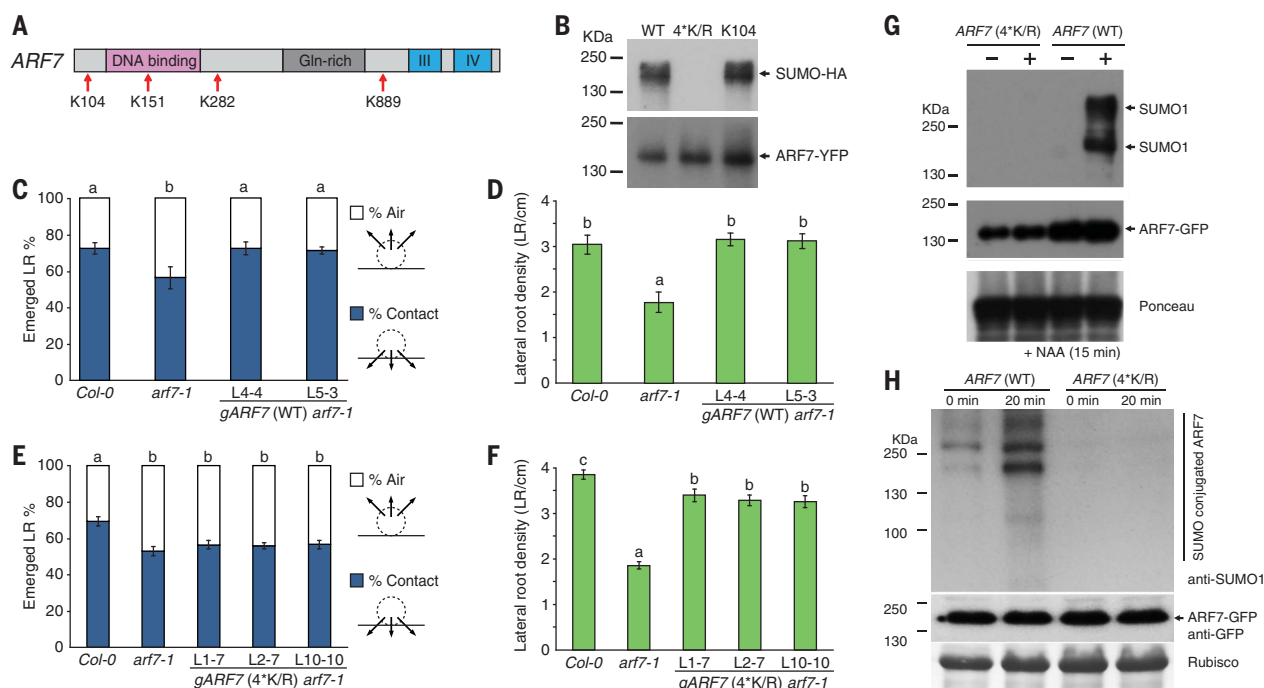
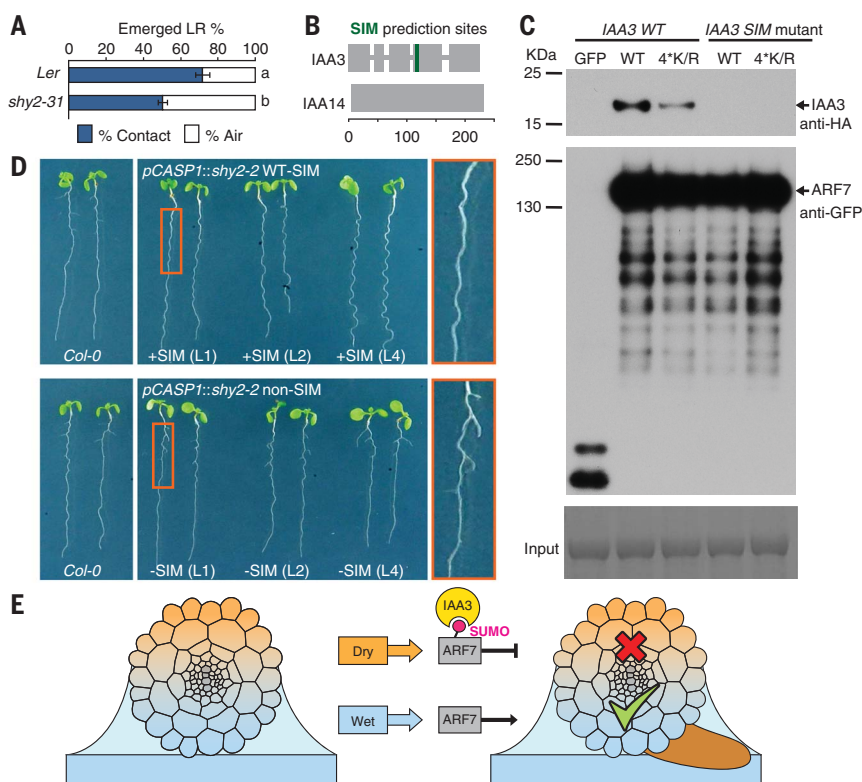


Fig. 2. ARF7 SUMOylation regulates hydropatterning and DNA binding affinity. (A) Schematic of ARF7 domains and four predicted SUMO sites K104, K151, K282, and K889. (B) Replacing all ARF7 SUMO site lysine with arginine residues in ARF7-GFP(4*K/R) blocks SUMOylation with HA-SUMO1 (but not WT ARF7 or single SUMO K104) in transient expression assays. YFP, yellow fluorescent protein. (C and D) Bioassays reveal that two independent transgenic lines expressing WT gARF7 can rescue *arf7-1* hydropatterning (C) and LR density defects (D). *n* LR = 196 (Col-0), 78 (*arf7-1*), 292 (L4-4), and 231 (L5-3); *n* plants = 7 (Col-0), 5 (*arf7-1*), 10 (L4-4), and 9 (L5-3).

(E and F) Bioassays reveal that three independent transgenic lines expressing gARF7(4*K/R) cannot rescue *arf7-1* hydropatterning (E) but do restore LR density (F). *n* LR = 374 (Col-0), 268 (*arf7-1*), 198 (L1-7), 286 (L2-7), and 206 (L10-10); *n* plants = 12 (Col-0), 16 (*arf7-1*), 8 (L4-4), 11 (L5-3), and 8 (L10-10). Data are mean values \pm SE, and statistics were performed as in Fig. 1C. (G) Immunoprecipitation reveals that ARF7-GFP [but not ARF7-GFP(4*K/R)] is rapidly SUMOylated 15 min after naphthaleneacetic acid (NAA) treatment. (H) Immunoprecipitation reveals that ARF7-GFP [but not ARF7-GFP(4*K/R)] is rapidly SUMOylated 20 min after seedlings were removed from their agar plates.

Fig. 3. SHY2 interacts with ARF7 in a SUMO-dependent manner to control hydropatterning.

(A) Bioassay reveals that *IAA3*/SHY2 mutant allele *shy2-31* does not exhibit a hydropatterning response. Data shown are mean \pm SE. Letters indicate a significant difference compared with WT (*Ler*) roots based on Student's *t* test ($P < 0.05$). *n* LR = 208 (*Ler*) and 604 (*shy2-31*); *n* plants = 7 (*Ler*) and 19 (*shy2-31*). (B) The *IAA3* (but not *IAA14*) sequence contains a putative SIM, suggesting that *IAA3* could bind SUMOylated ARF7. (C) Transient expression of *IAA3*/SHY2-HA (WT-SIM) or *IAA3*/SHY2-HA (SIM mutant) with ARF7-GFP or ARF7-GFP(4*K/R), followed by immunoprecipitation and western analysis, revealed that *IAA3* interacts with ARF7 in a SIM- and SUMO-dependent manner. (D) Phenotyping *Arabidopsis* seedlings expressing *shy2-2* \pm SIM by using the endodermal *CASP1* promoter revealed *CASP1:shy2-2* (WT) blocks LR branching (top), whereas *CASP1:shy2-2* (non-SIM) branch normally (bottom). Seedlings are from six independent lines termed SIM-containing *CASP1:shy2-2* (WT L1, L2, and L3) and non-SIM-containing *CASP1:shy2-2* (SIML1, L2, and L3). (E) Schematic summarizing the SUMO-dependent ARF7 model for hydropatterning, in which ARF7 is SUMOylated on the air side of the root, resulting in an interaction with *IAA3* that inhibits LR initiation. On the contact side of the root, ARF7 is not SUMOylated, enabling the transcriptional factor to activate expression of genes involved in LR initiation.



Our study has revealed how environmental inputs modulate the auxin response machinery. The SUMO-mediated posttranslational regulation of auxin signaling operates on top of the specificity provided from distribution of the hormone itself and the expression patterns of individual regulatory components. Thus, auxin regulation controls root branching pattern in response to water availability, building a root architecture that optimizes access to water.

REFERENCES AND NOTES

1. A. Hodge, *New Phytol.* **162**, 9–24 (2004).
2. B. D. Gruber, R. F. H. Giehl, S. Friedel, N. von Wirén, *Plant Physiol.* **163**, 161–179 (2013).
3. E. C. Morris *et al.*, *Curr. Biol.* **27**, R919–R930 (2017).
4. Y. Bao *et al.*, *Proc. Natl. Acad. Sci. U.S.A.* **111**, 9319–9324 (2014).
5. N. E. Robbins 2nd, J. R. Dinneny, *Proc. Natl. Acad. Sci. U.S.A.* **115**, E822–E831 (2018).
6. J. Lavenus *et al.*, *Trends Plant Sci.* **18**, 450–458 (2013).
7. T. Ulmasov, J. Murfett, G. Hagen, T. J. Guilfoyle, *Plant Cell* **9**, 1963–1971 (1997).
8. Y. Okushima *et al.*, *Plant Cell* **17**, 444–463 (2005).
9. R. M. Harper *et al.*, *Plant Cell* **12**, 757–770 (2000).
10. M. A. Moreno-Risueno *et al.*, *Science* **329**, 1306–1311 (2010).
11. B. Péret *et al.*, *Nat. Cell Biol.* **14**, 991–998 (2012).
12. J. Lavenus *et al.*, *Plant Cell* **27**, 1368–1388 (2015).
13. T. Goh, S. Joi, T. Mimura, H. Fukaki, *Development* **139**, 883–893 (2012).
14. E. S. Johnson, *Annu. Rev. Biochem.* **73**, 355–382 (2004).
15. D. R. Boer *et al.*, *Cell* **156**, 577–589 (2014).
16. T. Goh, H. Kasahara, T. Mimura, Y. Kamiya, H. Fukaki, *Philos. Trans. R. Soc. Lond. B Biol. Sci.* **367**, 1461–1468 (2012).
17. K. Swarup *et al.*, *Nat. Cell Biol.* **10**, 946–954 (2008).
18. J. E. M. Vermeer *et al.*, *Science* **343**, 178–183 (2014).
19. L. Conti *et al.*, *Dev. Cell* **28**, 102–110 (2014).
20. L. Conti *et al.*, *Plant Cell* **20**, 2894–2908 (2008).

ACKNOWLEDGMENTS

We acknowledge T. Guilfoyle for insightful discussions and dedicate this manuscript in his memory. We thank J. Dewick for assisting with the submission of this manuscript and C. Testerink for providing seed for the *lbd16-2* mutant allele. **Funding:** This work was supported by awards from the Biotechnology and Biological Sciences Research Council (grants no. BB/G023972/1, BB/R013748/1, BB/L026848/1, BB/M018431/1, BB/PO16855/1, BB/M001806/1, BB/M012212); European Research Council (ERC) FUTUREROOTS Advanced grant 294729; ERC SUMOrice Consolidator grant 310235; Leverhulme Trust grant RPG-2016-409; ANR 2014-CE11-0018 Serrations grant; AuxID PICS grant from the CNRS; a joint INRA/University of Nottingham PhD grant to J.T.;

J.E.M.V. is supported by the Swiss National Science Foundation (PP00P3_157524 and 316030_164086) and the Netherlands Organization for Scientific Research (NWO 864.13.008). H.F. was supported by a Grant-in-Aid for Scientific Research on Priority Areas (19060006) from the MEXT, Japan. **Author contributions:** B.O.-P., N.L., D.v.W., J.B., K.H., H.F., J.E.M.V., T.V., J.R.D., A.P.F., A.B., A.S., and M.J.B. designed experiments; B.O.-P., N.L., D.v.W., J.B., A.K.S., K.H., J.T., R.B., E.M., M.S., B.K., and T.G. performed experiments; and B.O.-P., N.L., D.v.W., A.B., A.S., and M.J.B. wrote the manuscript. **Competing interests:** Authors declare no competing interests. **Data and materials availability:** No restrictions are placed on materials, such as materials transfer agreements. Details of all data, code, and materials used in the analysis are available in the main text or the supplementary materials.

SUPPLEMENTARY MATERIALS

www.sciencemag.org/content/362/6421/1407/suppl/DC1
Materials and Methods
Figs. S1 to S22
Tables S1 to S3
References (21–28)
Movie S1

19 June 2018; accepted 6 November 2018
10.1126/science.aau3956

Root branching toward water involves posttranslational modification of transcription factor ARF7

Beatriz Orosa-Puente, Nicola Leftley, Daniel von Wangenheim, Jason Banda, Anjil K. Srivastava, Kristine Hill, Jekaterina Truskina, Rahul Bhosale, Emily Morris, Moumita Srivastava, Britta Kumpers, Tatsuaki Goh, Hidehiro Fukaki, Joop E. M. Vermeer, Teva Vernoux, José R. Dinneny, Andrew P. French, Anthony Bishopp, Ari Sadanandom and Malcolm J. Bennett

Science **362** (6421), 1407-1410.
DOI: 10.1126/science.aau3956

Rooting out the mechanism of asymmetry

Plant roots grow not in response to architectural blueprints but rather in search of scarce resources in the soil. Orosa-Puente *et al.* show why a new lateral root emerges on the damp side of a root rather than the dry side (see the Perspective by Giehl and von Wirén). The transcription factor ARF7 is found across the whole root but acquires a posttranslational modification on the dry side of the root, which represses its function. ARF7 on the damp side remains functional and is thus able to initiate the signaling cascade that leads to a new lateral root.

Science, this issue p. 1407; see also p. 1358

ARTICLE TOOLS

<http://science.sciencemag.org/content/362/6421/1407>

SUPPLEMENTARY MATERIALS

<http://science.sciencemag.org/content/suppl/2018/12/19/362.6421.1407.DC1>

RELATED CONTENT

<http://science.sciencemag.org/content/sci/362/6421/1358.full>

REFERENCES

This article cites 28 articles, 11 of which you can access for free
<http://science.sciencemag.org/content/362/6421/1407#BIBL>

PERMISSIONS

<http://www.sciencemag.org/help/reprints-and-permissions>

Use of this article is subject to the [Terms of Service](#)

Science (print ISSN 0036-8075; online ISSN 1095-9203) is published by the American Association for the Advancement of Science, 1200 New York Avenue NW, Washington, DC 20005. The title *Science* is a registered trademark of AAAS.

Copyright © 2018 The Authors, some rights reserved; exclusive licensee American Association for the Advancement of Science. No claim to original U.S. Government Works